Toward the Insulin−IGF-I Intermediate Structures: Functional and Structural Properties of the [Tyr^{B25}NMePhe^{B26}] Insulin Mutant†

Lenka Žáková,‡ Jiří Brynda,§ Oskar Au-Alvarez,|| Eleanor J. Dodson,⊥ Guy G. Dodson,⊥ Jean L. Whittingham,⊥ and Andrzej M. Brzozowski*,⊥

Department of Biological Chemistry, Institute of Organic Chemistry and Biochemistry, Academy of Sciences of the Czech Republic, Flemingovo 2, 166 10 Prague, Czech Republic, Institute of Molecular Genetics, Academy of Sciences of the Czech Republic, Flemingovo 2, 166 10 Prague, Czech Republic, Departamento de Quimica, Facultia De Cienicias Naturales, Universidad de Oriente, Santiago de Cuba 90500, Cuba, and York Structural Biology Laboratory, Department of Chemistry, University of York, York YO10 5YW, U.K.

Received June 3, 2004; Revised Manuscript Received September 13, 2004

ABSTRACT: The origins of differentiation of insulin from insulin-like growth factor I (IGF-I) are still unknown. To address the problem of a structural and biological switch from the mostly metabolic hormonal activity of insulin to the predominant growth factor activities of IGF-I, an insulin analogue with IGF-I-like structural features has been synthesized. Insulin residues Phe^{B25} and Tyr^{B26} have been swapped with the IGF-I-like Tyr^{24} and Phe^{25} sequence with a simultaneous methylation of the peptide nitrogen of residue Phe^{B26}. These modifications were expected to introduce a substantial kink in the main chain, as observed at residue Phe^{25} in the IGF-I crystal structure. These alterations should provide insight into the structural origins of insulin−IGF-I structural and functional divergence. The [Tyr^{B25}NMePhe^{B26}] mutant has been characterized, and its crystal structure has been determined. Surprisingly, all of these changes are well accommodated within an insulin R6 hexamer. Only one molecule of each dimer in the hexamer responds to the structural alterations, the other remaining very similar to wild-type insulin. All alterations, modest in their scale, cumulate in the C-terminal part of the B-chain (residues B23−B30), which moves toward the core of the insulin molecule and is associated with a significant shift of the A1 helix toward the C-terminus of the B-chain. These changes do not produce the expected bend of the main chain, but the fold of the mutant does reflect some structural characteristics of IGF-1, and in addition establishes the CO^{A19}−NH^{B25} hydrogen bond, which is normally characteristic of T-state insulin.

Despite a wealth of structural information about human insulin, the exact nature of the binding of this hormone to its cognate insulin receptor remains unknown. Some complementary data about the structure−function relationship of insulin come from studies on human insulin-like growth factor I (hIGF-I).[1] hIGF-I, as opposed to two-chain insulin, is a single polypeptide 70-amino acid hormone with close structural and biological connections to insulin, reflected in its ability to bind to both the hIGF-I receptor and, with lower affinity, the insulin receptor. Insulin consists of two disulfide-linked chains (residues A1−A21 and B1−B30), where the B-chain is homologous with the amino-terminal 29-residue region of hIGF-I. A 12-amino acid linking sequence ("C-loop") of hIGF-I joins its B-domain to a region corresponding to the A-chain of insulin. The terminus of the C-end of hIGF-I contains eight additional amino acids named the D-domain (Figure 1).

The comparative studies of insulin, IGF-I, and their analogues are complicated further by the ability of insulin to form at least two, different hexamer (T6 and R6) conformers. The so-called T (tense) state occurs when the A and B chains form a more compact molecule with the first six N-terminal residues (B1−B6) adopting an extended chain fold. In the R (relaxed) conformer, all these residues are in a fully α-helical conformation extending the already existing B9−B19 α-helix (*1*). However, several other intermediate T → R hexamers and insulin forms (e.g., T3R3 and T3R3^f) have also been observed (*2*)

Recent crystal structure determinations of hIGF-I (*3*, *4*) revealed a structure that might represent one of the active

† The work of L.Ž. and J.B. was supported by Research Project Z4 055 905, N° K5011112 awarded by the Academy of Sciences of the Czech Republic and the Center for Molecular and Gene Biotechnoloy supported by the Czech Ministry of Education (code LN00B030).

* To whom correspondence should be addressed. E-mail: marek@ysbl.york.ac.uk. Telephone: +44-(0)1904-328265. Fax: +44-(0)1904-328266.

‡ Institute of Organic Chemistry and Biochemistry, Academy of Sciences of the Czech Republic.

§ Institute of Molecular Genetics, Academy of Sciences of the Czech Republic.

|| Universidad de Oriente.

⊥ University of York.

[1] Abbreviations: hIGF-I, human insulin-like growth factor I; TPCK-trypsin, trypsin treated with L-1-tosylamine-2-phenylethyl chloromethyl ketone; DOI, desoctapeptide$^{B23-B30}$ insulin; Tris, TRIZMA buffer; Fmoc, 9-fluorenylmethoxycarbonyl; HBTU, 2-(1*H*-benzotriazol-1-yl)-1,1,3,3-tetramethyluronium hexafluorophosphate; DIPEA, diisopropylethylamine; PyBroP, bromo tris(pyrrolidinophosphonium) hexafluorophosphate; TFE, trifluoroethanol; DCM, dichloromethane; TFA, trifluoroacetic acid; TIS, triisopropylsilane; DMF, *N*,*N*-dimethylformamide; GFYNMeFTPK(Pac)T, Gly-Phe-Tyr-NMePhe-Thr-Pro-Lys(Pac)-Thr; Pac, phenylacetyl group; RP-HPLC, reverse phase high-performance liquid chromatography; SEM, standard error of the mean.

10.1021/bi048856u CCC: $27.50
Published on Web 11/25/2004

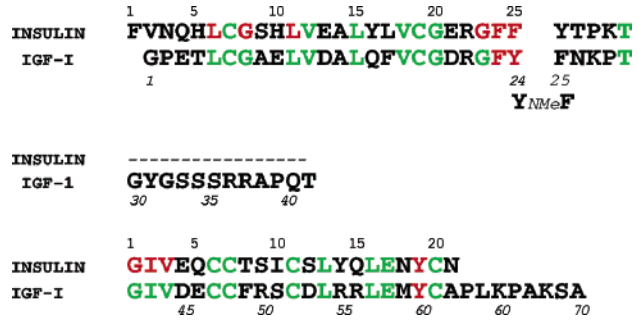

FIGURE 1: Sequence and chain organization of the [Tyr^{B25}NMePhe^{B26}] mutant, insulin, and hIGF-I. The sequence changes in [Tyr^{B25}NMePhe^{B26}] are given in the bottom part of the top row (B-chain) [otherwise, the mutant sequence has been omitted in the middle (C-chain) and bottom (A-chain) rows as it is identical to that of insulin]. The top numbering in each row corresponds to insulin and the bottom one to the IGF-I sequence. Identical residues in insulin and IGF-I are colored green, and residues that are important for receptor binding are colored red.

conformations of insulin adopted upon receptor binding. This interaction is known to involve the N-terminal part of the A-chain of insulin uncovered by the displacement of the B-chain C-terminus. However, the molecular bases of the structural switch that determine biological specificities of both hormones are still unknown. The putative "insulin-active" conformation described in hIGF-I is promoted by the C-loop which introduces a sharp bend at residue Phe^{25}, exposing residues 42−44 (equivalent to residues A1−A3 in insulin). This observation is in agreement with other studies, which have established the link between exposure of residues A1−A3 and insulin activity (*5*−*7*). On the other hand, there is other evidence (*8*−*11*) which demonstrates that not only the rigid, covalent bond between the N-terminus of the A-chain and the C-terminus of the B-chain but also an excessive flexibility of C-terminal residues of the B-chain leads to a low binding affinity of such insulin analogues. The three evolutionarily conserved aromatic residues, Phe^{B24}, Phe^{B25}, and Tyr^{B26} of insulin and Phe^{23}, Tyr^{24}, and Phe^{25} of hIGF-I, are among the most important residues for the interaction with insulin or IGF-I receptors (*12*−*14*). The alterations of these amino acids (especially those diminishing the hydrophobic character of these side chains) drastically affect the affinity of the hormones for their receptors (*15*).

Both the insulin and IGF-I receptors belong to the tyrosine kinase family of receptors with sequence homologies varying from 41 to 84% between different domains and subunits (*16*, *17*). Despite this high degree of similarity and analogous functional organizations of these receptors, insulin and IGF-I bind to the noncognate receptor with low affinity (*18*). The insulin−IGF-I mutant studies indicated also that their level of binding to the noncognate receptor is proportional to the degree of similarity of a particular analogue to the physiological ligand (*14*, *19*).

These observations pushed us toward a more detailed analysis of the possible "IGF-like" structural transitions within the insulin molecule. In this study, we have tried to probe the structural effects of swapping insulin residues Phe^{B25} and Tyr^{B26} with the IGF-I-like Tyr^{24} and Phe^{25} residues, respectively, coupled with the methylation of the main chain nitrogen atom of residue B26 (Figure 1). This additional modification of the main chain was introduced with the aim of forcing the terminal part of the B-chain of insulin to move away into an IGF-like conformation, mimicking the kink in IGF-I at residue Phe^{B25}. This new insulin mutant will here be termed [Tyr^{B25}NMePhe^{B26}]. The corresponding chain numberings in insulin (or the [Tyr^{B25}NMePhe^{B26}] mutant) and h-IGF-I are given in brackets and braces, respectively.

MATERIALS AND METHODS

Synthesis of the [Tyr^{B25}NMePhe^{B26}] Mutant

The preparation of [Tyr^{B25}NMePhe^{B26}] involved several steps. First, zinc-free porcine insulin was treated with TPCK-trypsin dissolved in 0.1 M $CaCl_2$ to give desoctapeptide$^{B23-B30}$ insulin (DOI). Second, DOI was coupled with the Tyr^{B25}NMePhe^{B26} octapeptide C-terminal analogue of the human insulin B chain, and finally, the protecting groups were removed.

Preparation of Desoctapeptide$^{B23-B30}$ Insulin (DOI)

To a solution of Zn-free porcine insulin (*20*) dissolved in 0.05 M Tris-HCl buffer (pH 9.0−9.2) was added TPCK-trypsin in 0.1 M $CaCl_2$ to a final enzyme:substrate ratio of 1:50. This solution was left for 20 h at room temperature, after which the pH of the solution was adjusted to 5.4 using 1 M HCl. The solution was then centrifuged at 2000*g* for 20 min, and the resulting supernatant was lyophilized. The lyophilized desoctapeptide insulin was subsequently dissolved in 10% acetic acid and purified by gel filtration using a Sephadex G50 matrix. This procedure yielded 75% pure desoctapeptide$^{B23-B30}$ insulin.

Preparation of the Gly-Phe-Tyr-NMePhe-Thr-Pro-Lys(Pac)-Thr-OH Octapeptide

The octapeptide analogue of the C-terminus of the human insulin B-chain was synthesized on a 2-chlorotrityl chloride resin. This process employed the Fmoc protection strategy for α-amino groups of individual amino acids, with *tert*-butyl group protection for the side chain of the tyrosine and threonine residues and phenylacetyl (Pac) group protection for the lysine residue. Coupling of the amino acids was carried out in a HBTU/DIPEA environment, with the exception of that of the *N*-methylphenylalanine, which was carried out in a PyBroP/DIPEA solution. The resulting peptide was cleaved from the resin using an acetic acid/TFE/DCM mixture (1:1:8 by volume), and the protecting groups of the sides were cleaved off using a TFA/TIS/H_2O/DCM solution (50:2:2:46 by volume), with the exception of phenylacetyl, which was removed later. The final yield was 85%.

Enzymatic Semisynthesis of the Insulin Analogue

The synthesis of the analogue was performed according to the method of Inouye (*21*, *22*). The amino component [G-F-Y-NMeF-T-P-K(Pac)-T, 150 mM] and 30 mM DOI were dissolved in a solution containing 55% (v/v) DMF, 10 mM $CaCl_2$, and TPCK-trypsin (enzyme:substrate molar ratio of 1:50), to a total volume of 200 μL. The pH value was adjusted to pH 6.9−7.0 using *N*-methylmorpholine. The resulting mixture was then incubated for 4−7 h at room temperature. The reaction, monitored by analytical RP-HPLC, was stopped by the addition of cold acetone. The

resulting sediment was diluted in 10% acetic acid and analyzed by preparative RP-HPLC. All peaks were collected and lyophilized, giving an overall yield of 10−15%.

Deprotection of the Insulin Analogue by Penicillin Amidohydrolase

The insulin analogue with the ϵ-amino group of Lys^{B29} protected by Pac was dissolved in 0.05 M phosphate buffer (pH 7.6) (*12*). Immobilized penicillin amidohydrolase was swelled in 0.05 M phosphate buffer for 30 min, and then the analogue was added. The reaction was allowed to run for 2.5 h, and then two peaks arising from RP-HPLC analysis were collected and lyophilized, giving a final of [Tyr^{B25}NMePhe^{B26}] yield of 50−60%.

Biological Assays

The assay described by Zorad *et al*. (*24*) was used to determine the relative binding affinities of insulin and [Tyr^{B25}NMePhe^{B26}] for the insulin receptor of rat adipose tissue plasma membranes. The membranes were isolated from epidymal fat of male rats (Wistar, 210−250 g); 50 μg of plasma membrane was incubated in a 5 mL test tube with [^{125}I]insulin (2×10^{-10} M $\sim$ 70 000 cpm). Then various concentrations of insulin or the insulin analogue (ranging from 10^{-13} to 10^{-6} M) in a buffer consisting of 2 mM *N*-ethylmaleimide, 13.2 mM $CaCl_2$, 0.1% (w/v) bovine serum albumin, and Tris-HCl (pH 7.6) were added to a total volume of 250 μL. Each solution was incubated for 21 h at 4 °C, and then the reaction was terminated by the addition of ice-cold 120 mM NaCl followed by a quick filtration on a Brandell (Gaithersburg, MD) cell harvester. The bound radioactivity was determined by γ-counting. Total binding (in the absence of unlabeled insulin) was ~10% of the total radioactivity. Nonspecific binding (in the presence of 10^{-5} M insulin) amounted to less than 15% of the total binding.

Analysis of the Binding Data

The relative receptor binding potencies of the insulin analogue were determined by measuring the concentration of the analogue causing half-maximal inhibition (IC_{50}) of labeled insulin binding and the concentration of standard human insulin causing the equivalent inhibition within a single experiment. Competitive binding curves were plotted using Graph-Pad (San Diego, CA) Prizm 3, comparing the best fit for single-binding site models. Relative receptor binding potency is defined as (IC_{50} value of human insulin)/(IC_{50} value of analogue) $\times$ 100.

Crystallization

[Tyr^{B25}NMePhe^{B26}] was crystallized by the hanging drop vapor diffusion method. Several attempts to crystallize the mutant using new protocols, different from pre-established crystallization methods for insulin, were unsuccessful. Eventually, crystals were obtained from drops consisting of 1 μL of protein solution (10 mg/mL analogue in 0.02 M HCl) and 1 μL of the reservoir solution [0.1 M trisodium citrate, 0.02% (w/v) zinc acetate, 6% (w/v) Tris-HCl buffer (pH 8.2)] suspended over 1 mL reservoirs. Different concentrations of phenol 0.05, 0.10, and 0.15% (w/v) were added to the reservoir solution prior to mixing with the protein. Crystals grew in all wells within 1 week. They belong to the $P2_1$ space group with one hexamer in the asymmetric unit (Matthews coefficient of 2.38 Da Å^{-3}, solvent content of 48%).

Table 1: X-ray Data and Refinement Statistics

Data Processing Statistics	
data collection site	in-house
wavelength (Å)	1.54
space group	$P2_1$
unit cell dimensions	$a = 59.90$ Å, $b = 62.12$ Å, $c = 47.80$ Å, $\beta = 110.6°$
diffraction limits (Å)	25.56−2.08 (2.19−2.08)[g]
no. of observations	96148
no. of unique reflections	17496
completeness of the data (%)	88.1 (89.2)[g]
R_{merge}[a]	3.4 (12.0)[g]
$I/\sigma\langle I\rangle$	5.7 (1.8)[g]
Refinement Statistics	
resolution range (Å)	25.57−2.08
no. of reflections used (R_{free} set)	17491 (956)
R_{cryst} (%)/R_{free}[b]	18.9/25.6
no. of protein atoms/ water molecules/metal ions	2475/83/2
rmsd for bonds (Å)/angles (deg)[c]	0.018/1.7
rmsd for main chain ΔB (Å)[d]	1.16
mean *B*-factor (Å^2)[e]	43.3/56.3/27.1/59.1/
% A, B, L/a, b, l, p/XX[f]	94.4/4.8/0.8

[a] $R_{merge} = 100\sum|I - \langle I\rangle|/\sum\langle I\rangle$. [b] $R_{crys} = \sum|F_{obs} - F_{calc}|/\sum F_{obs}$. R_{free} is like R_{cryst} but calculated over 5.2% of data that were excluded from the refinement process. [c] Root-mean-square deviations in bond lengths and angles from Engh and Huber ideal values. [d] Root-mean-square deviations between $B_{factors}$ for bonded main chain atoms. [e] Mean temperature factor for the whole molecule, main chain, side chain, metal, and water atoms, respectively. [f] Percentage of residues located in the most favored, additional allowed, and disallowed regions of the Ramachandran plot as determined by PROCHECK (*33*). [g] Highest-resolution shell statistics given in parentheses.

X-ray Crystallography

Data Collection. As the crystals were found to be extremely sensitive to changes in the crystallization environment, flash-cooling experiments were unsuccessful. Therefore, a 2.08 Å resolution data set was collected at room temperature from a crystal mounted in a quartz capillary tube on in-house X-ray equipment (mar345 Image Plate Detector, Nonius FR 591 generator) using Cu Kα_1 radiation. All data were integrated and reduced using MOSFLM (*25*). X-ray data collection and processing statistics are summarized in Table 1.

Structure Determination and Refinement. The insulin coordinates of Protein Data Bank entries 1EVR and 1EV6 (*26*) with the water molecules removed were used as models in a preliminary search in MOLREP (*27*). Slightly better results were obtained with 1EVR, which was subsequently used in final search in AMoRe (*28*) (used here due to its more powerful rigid body refinement tool) to determine the structure by molecular replacement. Final restrained and rigid body refinements were performed with REFMAC5 (*29*) employing maximum likelihood procedures. NCS restraints were not imposed during any stages of the refinement. Water molecules were located using ARP/warp (*30*). Successive rounds of refinement using all data between 25.57 and 2.08 Å, in conjunction with manual rebuilding, gave a final model with an R_{cryst} of 18.9% and an R_{free} of 24.9%. The final model comprises 2409 protein atoms, two metal atoms, and 83 water

Table 2: Values of IC_{50}[a] and Receptor Binding Affinities[b] of Insulin and the [$Tyr^{B25}NMePhe^{B26}$] Insulin Mutant

ligand	$IC_{50} \pm$ SEM (nM)	*n*	potency (%)
human insulin	1.83 ± 1.18	10	100
[$Tyr^{B25}NMePhe^{B26}$] insulin	7.82 ± 1.95	4	23

[a] IC_{50} values represent concentrations of insulin or the insulin analogue causing half-maximal inhibition of binding of [^{125}I]insulin to the insulin receptor. Each value represents the mean $\pm$ SEM of multiple determinations; the number of separate determinations is shown in parentheses. [b] Relative receptor binding affinity defined as (IC_{50} of human insulin)/(IC_{50} of analogue) $\times$ 100. See Experimental Procedures for details.

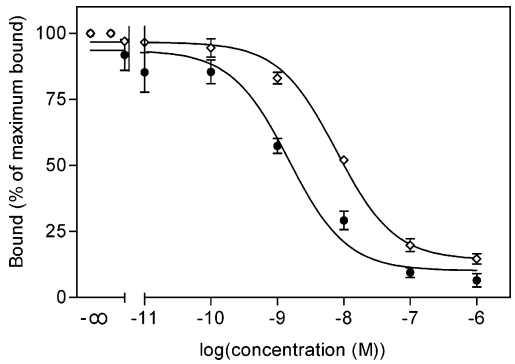

FIGURE 2: Inhibition of binding of [^{125}I]insulin to rat adipose tissue plasma membranes by human insulin (●) and [$Tyr^{B25}NMePhe^{B26}$] insulin (◇). Values are means $\pm$ SEM. See Experimental Procedures for details. Quantitative information is provided in Table 2.

molecules. All model building was carried out using QUANTA (QUANTA98, Accelrys Inc., San Diego, CA). Programs of the CCP4 suite (*31*) were used during the structure solution and refinement. A summary of the refinement statistics is given in Table 1. Superpositions of [$Tyr^{B25}NMePhe^{B26}$] and insulin and hIGF-I were carried out using QUANTA with the insulin [B9−B19] helix ({B8−B19} of IGF-I) as the main template. Figures 3 and 5 were produced using MOLSCRIPT (*32*), and Figures 4, 6, and 7 were created using QUANTA. The atomic coordinates of the final model have been deposited in the Protein Data Bank as entry 1W8P.

RESULTS AND DISCUSSION

Biological Activity of the [$Tyr^{B25}NMePhe^{B26}$] Mutant. The insulin receptor binding affinity of [$Tyr^{B25}NMePhe^{B26}$] insulin is only 25% of that of human insulin (Table 2 and Figure 2). Previous studies of the replacement of Phe^{B25} with tyrosine have already shown a small decrease in the binding potency (*12*). The substitution of the hydrogen atom of the amide nitrogen with an *N*-methyl group in [$Tyr^{B25}NMePhe^{B26}$] insulin eliminates its ability to form one of the β-strand hydrogen bonds required for dimer formation. However, the retention of full receptor affinity by despentapeptide$^{B26-B30}$ insulin-B25-amide (*34*, *35*) suggests that this hydrogen bond is not crucial for interaction with the insulin receptor (*8*), although the potential involvement of the [B25] amide group in this insulin bond in forming a hydrogen bond with [A19] cannot be ruled out.

The C-terminus of the B-chain of insulin is extremely sensitive to any conformational alteration of the backbone. Studies on insulin with [B24−B25/B25−B26] peptide bonds replaced with an ester bond (*36*, *37*) or a methylene group (*38*) showed extremely low receptor binding affinity, which could indicate a very high flexibility of this part of the molecule, which may cause its inability to be stabilized in an "active" conformation. The roles of [B25] and [B26] amides are likely to be substantially different as methylation of NH[B26] in destetrapeptide$^{B27-B30}$ insulin-B26-amide (DTIA) does not significantly affect its ability to bind to a IR or its biological activity, while [NMeB25]DTIA variants retain no more than 2.3% of the potency of human insulin in *in vitro* studies (*11*). On the contrary, the N-methylation of the [B26] peptide in DTIA associated with [B26]Tyr → His substitution gives rise to a potency of 5250%, yielding the most potent insulin ever obtained (*11*). Hence, the 25% potency of [$Tyr^{B25}NMePhe^{B26}$] is more likely to result from the converging and mutual effects of both the [Phe^{25} → Tyr] swap and the NMe[B26] methylation than from a particular single modification.

The discussion of these differing results will follow here a more detailed description of the [$Tyr^{B25}NMePhe^{B26}$] structure and the conformational changes found in the crystals of this mutant insulin.

Insulin, [$Tyr^{B25}NMePhe^{B26}$], and IGF-I Structural Relationships. In the discussion below, we analyze the structural relationships of the molecules (here termed *xz* forming one of the dimers of [$Tyr^{B25}NMePhe^{B26}$] with (a) its structural equivalents (*XZ*) from the monoclinic human insulin {for simplicity, here termed Wild Type, WT [PDB entry 1ZNJ (*39*)]} and (b) the single molecule of hIGF-I [PDB entry 1GZR (*4*)]). This particular (1ZNJ) insulin structure was chosen for a more detailed comparison because of its high degree of similarity in crystal packing with [$Tyr^{B25}NMePhe^{B26}$] ($a = 59.90$ Å, $b = 62.12$ Å, $c = 47.80$ Å, and $\beta = 110.6°$ for [$Tyr^{B25}NMePhe^{B26}$] vs $a = 61.23$ Å, $b = 61.65$ Å, $c = 48.05$ Å, and $\beta = 110.5°$ for insulin), to minimize the bias that could result from different interhexamer contacts. In addition, the 1ZNJ insulin model was also probed in the molecular replacement searches, giving solutions very comparable to the other models. The comparisons result from the alignments of these structures using part of their B helix, [Ser9]{Ala8}[Val18]{Val17}, as a template (Figure 3).

The structure of [$Tyr^{B25}NMePhe^{B26}$] in this crystal is similar to that of the R6 insulin with three dimers assembled into a hexameric 32 organization. There are two zinc ions on the 3-fold axis, each tetrahedrally coordinated to three histidines and one water molecule. The formation of the R6 hexamer in [$Tyr^{B25}NMePhe^{B26}$] was likely to be due to the presence of phenol in the crystallization medium. Six phenols in the structure form hydrogen bonds, one to the carbonyl oxygen of [A6] and the other to the peptide nitrogen of [A11].

Inspection of [$Tyr^{B25}NMePhe^{B26}$] and WT hexamers (Figure 4) showed that the structural differences are not evenly propagated throughout these assemblies. However, the differences have local character and concern mostly the subtle changes of the conformation of the C-terminal part of the B-chain (the overall rmsd between the dimers of the mutant was less than 0.1 Å). All main new structural features such as $CO^{B25}-NH^{A19}$ hydrogen bond were fully preserved in all dimers (e.g., the length of this interaction varied from 2.79 Å, through 2.95 Å, to 3.1 Å). The *xz* dimer (equivalent of AB and CD chains in the PDB file) that exhibited the

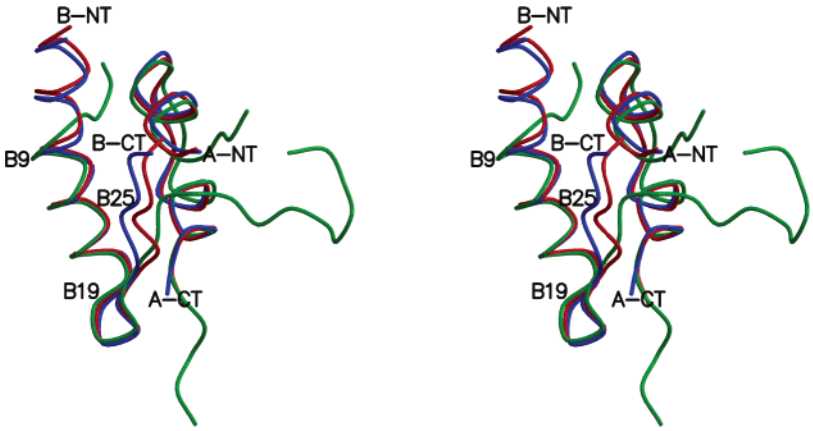

FIGURE 3: Stereoview of the main chain structure of [Tyr^{B25}NMePhe^{B26}] molecules [blue (*x*) and red (z)] superimposed on the [B9−B18] helix, with the hIGF-I structure in green (see Figure 4 for the definition of *x* and *z*).

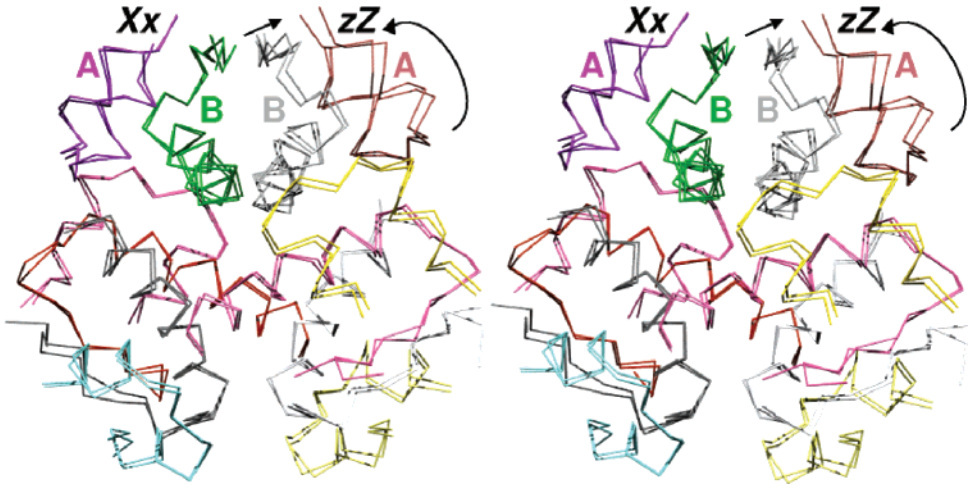

FIGURE 4: Comparison of the [Tyr^{B25}NMePhe^{B26}] hexamer with the wild-type monoclinic insulin structure [a certain nonstandard projection (3-fold hexamer axis not perpendicular to the plane of the figure) has been chosen to visualize differences in hexamer packing]. The molecules and dimers that are discussed in the text in more detail are marked as *xz* for [Tyr^{B25}NMePhe^{B26}] and *XZ* for the wild-type insulin; A and B refer to A- and B-chains, respectively, of insulin. The arrows show the direction of movements within B- and A-chains (divergent stereo).

highest degree of conformational changes was used for further comparisons with its *XZ* equivalent from the WT crystal.

As both molecules of the *XZ* dimer of the WT structure are virtually identical (average rmsd on Cα atoms of ∼0.13 Å) only one comparison, with the *X* molecule, has been carried out.

Comparison of the [Tyr^{B25}NMePhe^{B26}] x Monomer with the X Molecule. The overall structures of the *x* and *X* molecules (Figure 4) are very similar, with the rmsd for Cα atoms being 0.31 Å. The conformations of practically all of the side chains of the N-terminus and the α-helix of the B-chain are very alike, with the rings of [B1]Phe, [B16]Phe, and [B24]Phe being virtually fully superimposable. Surprisingly perhaps, the methylation of the nitrogen atom from the peptide bond of Phe^{B26} does not produce any perturbation of the main chain in the *x* molecule.

The position of the new [B25]Tyr side chain is well-defined in the electron density map (Figure 5). It is situated between two alternative conformations of [B25]Phe found in the *X* molecule. The phenyl rings of the new [B26]Phe and WT [B26]Tyr occupy similar positions, wedged between [B12]Val and [B28]Pro. However, [B26]Phe of [Tyr^{B25}NMePhe^{B26}] has moved into the protein core by ca.

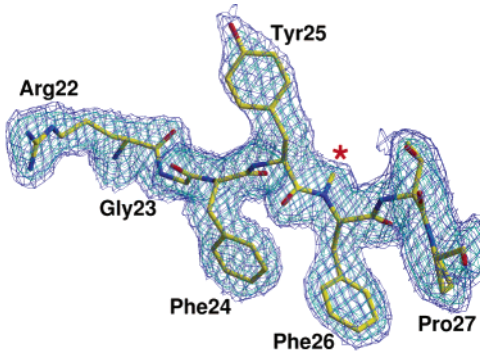

FIGURE 5: Electron density [1σ level (blue) and 0.5σ (purple)] of the [B22−B27] region. The position of methyl group present in the [B25]−[B26] peptide bond is marked with the red asterisk; residues are shown in stick representation with nitrogen, oxygen, and carbon atoms colored blue, red, and yellow, respectively.

1 Å (Figure 6). As the phenyl ring of [B26]Tyr sits in a fully hydrophobic environment in the WT molecule and is not (cannot be) engaged in any hydrogen bonds, this small displacement probably reflects more favorable surroundings for the new benzene side chain of [B26]Phe. The largest differences between the C-termini of the B-chain in *x* and *X* molecules (1.74 Å) are at the [B28]Pro Cα atoms, but the overall conformations of the B-chains here are very alike.

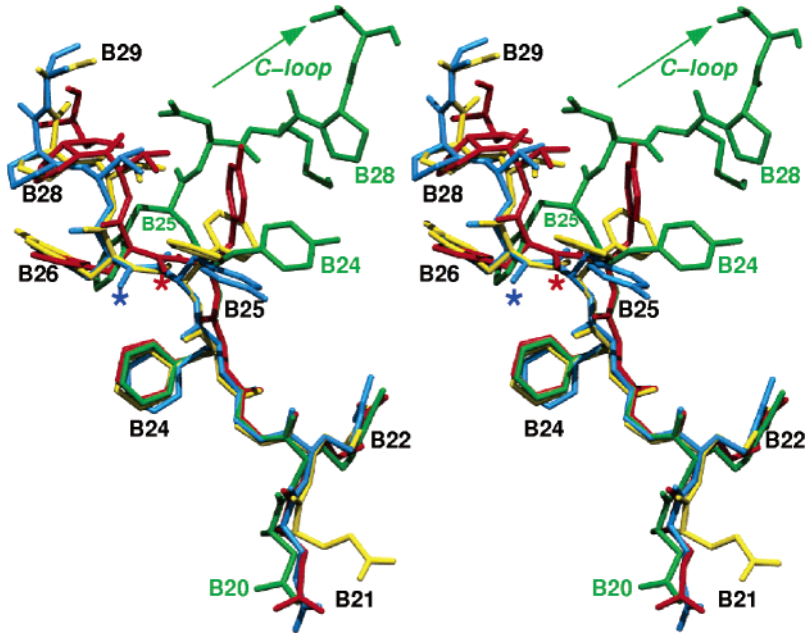

FIGURE 6: Stereoview (divergent) of C-terminal parts of the B-chain of *x* (blue), *z* (red), *X* (yellow), and hIGF-I (green) molecules. Blue and red asterisks are located next to the methyl groups of N[B26]; the green arrow shows the direction of the C-loop in hIGF-I.

The A1 helices in molecules *x* and *X* are almost identical. The A2 helix in molecule *x* shows small displacement toward the A1 helix of molecule *X*, reflected in the 0.63 Å distance between the Cα positions of A19 tyrosines. This movement, resulting also in stronger hydrogen bonding between [A19]Tyr and [A5]Gln (2.27 Å), is more pronounced in the *z* molecule.

Comparison of the [Tyr^{B25}NMePhe^{B26}] z Monomer with the x, X, and Z Molecules. In contrast to the *x* molecule, the *z* molecule of [Tyr^{B25}NMePhe^{B26}] insulin shows some interesting structural changes. First, the [B9−B18] α-helix overlaps less with its *x*, *X*, and *Z* counterparts (e.g., N-termini [B1]Phe residues are displaced by ca. 2 Å). The changes in the C-terminal part of the B-chain are already initiated at the beginning of its *β*-strand, and the position of the Cα atom of [B23]Gly deviates by 0.67 Å from that in its WT site. The [B24]Phe Cα atoms are also displaced, by 0.67 Å, while their phenyl rings occupy the same position. The maximum displacement of the main chain from its WT conformation in the *z* molecule occurs at the site of [B25]Tyr; its Cα atom is 1.87 Å from the WT position. As Figure 6 shows, the phenyl ring of [B25]Tyr is located between the alternative positions of this side chain found in molecules *X* and *Z* but opposite in direction to that seen in the *x* molecule.

Because of the large repositioning of its Cα atom, the phenolic ring of [B25]Tyr acquires a conformation almost perpendicular to the plane containing all of the [B25] aromatic rings in other insulin molecules (Figure 6).

The perturbation of the remaining part of the *z* molecule main B-chain continues further toward its C-terminus (by ca. 1 Å), but the side chains of [B26]Phe, [B27]Thr, and [B28]Pro maintain conformations similar to their *x*, *X*, and *Z* conformations. The methyl group is approximately 0.9 Å from the main chain of [B26]Phe. It is interesting that the overall changes of the C-terminal part of the B-chain and the general route of its displacement are not toward the "outer" side of the insulin molecule but are pushing the [B23−B29] polypeptide more toward the core of the insulin molecule and its A1 and A2 helices (see Figure 4). It is also interesting that these changes are coupled with a significant shift of the A1 helix toward the C-terminus of the B-chain, with the maximum displacement along the axis of the helix at the [A3]Val position (1.15 Å). This rearrangement puts [B29]Lys in close van der Waals contact with the [A1]Gly terminus. These changes are opposite to those resulting from the N-methylation of the [B26] nitrogen atom and the [B25−B26] Phe ↔ Tyr swap. Thus, the overall structural changes not only do not increase the mobility of the B-chain but also bring about an overall contraction and increased compactness of the insulin molecule.

Comparison of the Dimers and Hexamer of [Tyr^{B25}NMePhe^{B26}] and Human Insulin. The comparison of the dimers and hexamers is a complicated matter, and for simplicity, it involves here only the deviations in the region of the structure that is most affected by the introduction of the methyl group, i.e., those corresponding to the [B21−B29] polypeptides. The introduction of the methyl group provokes a displacement of these peptides away from the WT insulin position and toward the core of the molecule. However, this displacement is not the same in all of the dimers of the hexamer. As a measure of the displacement, we found that the distance between the Cα atoms at position 25 is greater for L25 and J25 (6.41 Å) followed by B25 and D25 (6.35 Å) and F25 and H25 (6.02 Å) (where B to L is the chain numbering in the final PDB file). In WT insulin, the corresponding distances are 4.38, 4.16, and 4.28 Å, respectively. The increased lengths of the new distances provoke the breaking of the intermolecular *β*-sheet in our structure (Figure 7). Only one of the four CO−NH hydrogen bonds of this *β*-sheet is almost preserved in the *z* molecule [CO−N, 3.43 Å (2.99 Å in WT)] at the [B26^{z}−B24^{x}] contact. The three remaining main chain−main chain hydrogen bonds are broken: [B26^{z}−B24^{x}], 4.09 Å (2.63 Å in the WT); [B24(CO)^{z}−B26^{x}], 4.42 Å (2.57 Å); and [B24(NH)^{z}−B26^{x}], 4.46 Å (3.00 Å).

Comparison of the [Tyr^{B25}NMePhe^{B26}] x and z Monomers with Human IGF-I. It was assumed that the methylation of the [B25] N peptide bond atom and the swap of [B25]Tyr

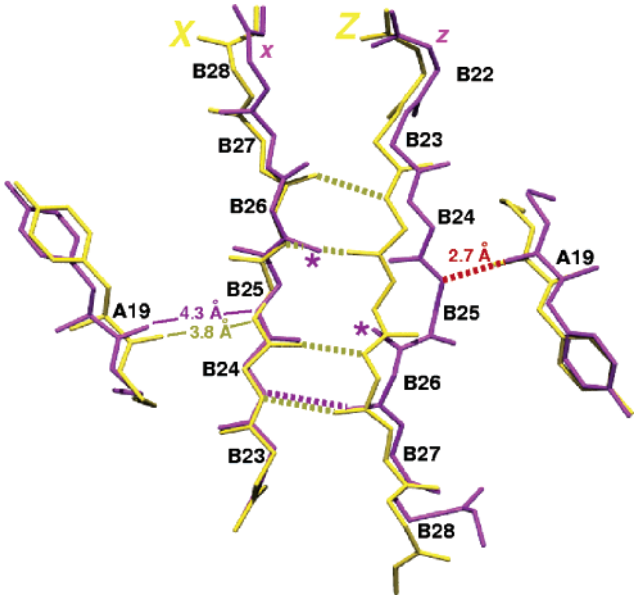

FIGURE 7: Effect of methylation (CH_3 marked with an asterisk) of peptide nitrogen atom of residue [B26] on the dimer/monomer hydrogen bond network: wild-type insulin (R-state) (*XZ* molecules) in yellow and [$Tyr^{B25}NMePhe^{B26}$] (*xz* molecules) in magenta. Distances in angstroms indicate the separations between the CO group of [A19] and the NH group of [B25]; the new [A19]−[B25] hydrogen bond in [$Tyr^{B25}NMePhe^{B26}$] (2.7 Å), typical for the T-state insulin and hIGF-I, is colored red.

and [B26]Phe for the typical IGF sequence of Phe and Tyr might produce a bend or distortion of the main chain at the [B26]{B25} Cα position, as seen in the IGF-I structure associated with its unique C-loop. Although this conformational change does not occur in [$Tyr^{B25}NMePhe^{B26}$], the position of the [B26]Phe Cα atom in the *z* molecule is nonetheless halfway between insulin-like and IGF-I-like conformations (Figure 6). One of the consequences of this motion is the introduction of a new hydrogen bond between the CO group of [A19] (one of the key residues for receptor binding) and the NH group of [B25] (2.79 Å), which also occurs in the hIGF-I (2.99 Å) structure but not in R-state molecule *x* (4.48 Å) or in molecules *X* and *Z* (3.81 Å) of insulin (see Figure 7) (the CO^{A19}−NH^{B25} distances in two other dimers of the mutant are 2.95 and 3.1 Å, respectively). This hydrogen bond (length usually in the range of 2.79−3.39 Å) is one of the characteristic structural features typical for T-state insulins and is adopted in [$Tyr^{B25}NMePhe^{B26}$] R-like hexamers by half of the protein molecules. In hIGF-I, this hydrogen bond is linked with other strong interactions between the C-terminus of the A-chain and the terminal fragment of the B-chain, and contributes significantly to the stabilization of the carboxyl part of the A2 helix, the conformation of the B-chain, and the rigidity of the C-neck region. It is tempting to see the emergence and strengthening (shortening) of the Phe^{B25}−Tyr^{A19} hydrogen bond as one of the potential sources of lower receptor affinity of the [$Tyr^{B25}NMePhe^{B26}$] mutant due to interference of this interaction with the conformational rearrangement of this region that is required for an effective receptor binding.

Although the B-chain in the *z* molecule does not bend in an IGF-I-like fashion, it seems that its distortion, due to the methylation of the [B26] N atom, leads to an even more stable conformation of this part of the molecule. This is in contrast to other insulin mutants, where modifications of the B-chain usually lead to higher mobility and local disorder (*7*−*9*).

In addition, the shift of the A1 helix in the *z* molecule parallels the overall shift of the A1 and A2 α-helices seen in hIGF-I. Although the key role of the IGF-I C-loop in generating compactness and rigidity of the region is clear, it is interesting that hIGF-like Phe ↔ Tyr swap at positions [B25] and [B26] and the methylation of the N atom of the residues at position [B26] have resulted in a more compact (IGF-like) structure in the insulin molecule.

To summarize, the [B25]Phe ↔ [B26]Tyr swap, coupled with the introduction of a methyl group on the [B26]N atom, has produced modest but significant changes in the C-terminal part of the B-chain. They result in a movement of the [B23−B29] polypeptide toward the core of insulin and its A1 and A2 helices, which is associated with a significant shift of the A1 helix toward the C-terminus of the B-chain. These changes do not produce the expected bend of the main chain at the [B26] Cα atom in hIGF-I-like fashion, but the fold of the mutant undergoes restructuring in that direction, resulting in an overall contraction of the molecule and the break of the main chain hydrogen bonds within the dimer. These results also support the observation that methylation of the [B26] peptide bond is not crucial for the insulin function and that the chemical character of the side chain [e.g., [B26Tyr → His] (*11*)] but not of the main chain (after [B26]) is more important for insulin potency.

The combination of chemical and sequence modifications in the [$Tyr^{B25}NMePhe^{B26}$] mutant illustrates the plasticity of the insulin molecule. In a general sense, it is interesting that the steric pressure introduced into the hexamer by the N−CH_3 bond at position [B26] has been accommodated by a similar adjustment within each of the 3-fold related dimers, and the 3-fold symmetry is thus well preserved. However, the adjustment does not reflect the local 2-fold symmetry; it moves only one main chain segment away from the *β*-sheet structure. With this, the NH^{B25}−CO^{A19} hydrogen bond, a feature of the T-state (the free dimer and two-Zn hexamer) insulin and hIGF-I, is restored. Similar heterogeneous responses of insulin aggregates to nonstandard modifications described here have also been observed in *allo*-Ile[A2] (*40*), where chiral perturbation was accommodated differently in T- and R-state insulin cores.

Our results indicate again the sophisticated complexity of the insulin molecule, which despite its very limited size, is capable of the accommodation of significant challenges coming from the chemical modifications of primary and main chain structures despite restraints of the hexamer assembly. The more unambiguous insight into the insulin−IGF-I structural relationship still requires further research, including the addition of more IGF-like sequence (e.g., [B28]Pro ↔ [B29]Lys swap) to the [$Tyr^{B25}NMePhe^{B26}$] mutant. This may provide some evidence about whether the [B28] ↔ [B29] residue swap, which has been shown to cause the monomerization of insulin (*41*), will be capable of promoting the hIGF-like conformational distortion of the B-chain of the insulin polypeptide.

REFERENCES

1. Kaarsholm, N. C., Ko, H. C., and Dunn, M. F. (1989) Comparison of solution structural flexibility and zinc-binding domains for

insulin, proinsulin, and miniproinsulin, *Biochemistry 28*, 4427−4435.
2. Ciszak, E., Beals, J. M., Frank, B. H., Baker, J. C., Carter, N. D., and Smith, G. D. (1995) Role of C-terminal B-chain residues in insulin assembly: The structure of hexameric $Lys^{B28}Pro^{B29}$-human insulin, *Structure 3*, 615−622.
3. Vajdos, F. F., Ultsch, M., Schaffer, M. L., Deshayes, K. D., Liu, J., Skelton, J., and de Vos, A. M. (2001) Crystal structure of human insulin-like growth factor-1: Detergent binding inhibits binding protein interactions, *Biochemistry 40*, 11022−11029.
4. Brzozowski, A. M., Dodson, E. J., Dodson, G. G., Murshudov, G., Verma, C., Turkenburg, J. P., de Bree, F. M., and Dauter, Z. (2002) Structural origins of the functional divergence of human insulin-like growth factor-I and insulin, *Biochemistry 41*, 9389−9397.
5. Xu, B., Hua, Q. X., Nakagawa, S. H., Jia, W., Chu, Y. C., Katsoyannis, P. G., and Weiss, M. A. (2002) Chiral mutagenesis of insulin's hidden receptor-binding surface: Structure of an allo-isoleucine (A2) analogue, *J. Mol. Biol. 316*, 435−441.
6. Derewenda, U., Derewenda, Z., Dodson, E. J., Dodson, G. G., Bing, X., and Markussen, J. (1991) X-ray analysis of the single chain B29-A1 peptide-linked insulin molecule. A completely inactive analogue, *J. Mol. Biol. 220*, 425−433.
7. Dodson, E. J., Dodson, G. G., Hubbard, R. E., and Reynolds, C. D. (1983) Insulin's structural behavior and its relation to activity, *Biopolymers 22*, 281−291.
8. Leyer, S., Gattner, H. G., Leithauser, M., Brandenburg, D., Wollmer, A., and Hocker, H. (1995) The role of the C-terminus of the insulin B-chain in modulating structural and functional properties of the hormone, *Int. J. Pept. Protein Res. 46*, 397−407.
9. Kurapkat, G., Siedentop, M., Gattner, H. G., Hagelstein, M., Brandenburg, D., Grotzinger, J., and Wollmer, A. (1999) The solution structure of a superpotent B-chain shortened single-replacement insulin analogue, *Protein Sci. 8*, 499−508.
10. Lenz, V., Gattner, H. G., Sievert, D., Wollmer, A., Engels, M., and Hocker, H. (1991) Semisynthetic des-(B27−B30)-insulins with modified B26-tyrosine, *Biol. Chem. Hoppe-Seyler 372*, 495−504.
11. Žáková, L., Barth, T., Jiráček, J., Barthová, J., and Zórad, S. (2004) Shortened insulins analogues: Marked changes in biological activity resulting from replacement of TyrB26 and N-methylation of peptide bonds in the C-terminus of the B-chain, *Biochemistry 43*, 2323−2331.
12. Mirmira, R. G., Nakagawa, S. H., and Tager, H. S. (1991) Importance of the character and configuration of residues of B24, B25, and B26 in insulin receptor interactions, *J. Biol. Chem. 266*, 1428−1436.
13. Nakagawa, S. H., and Tager, H. S. (1987) Role of the COOH-terminal B-chain domain in insulin-receptor interactions. Identification of perturbations involving the insulin main chain, *J. Biol. Chem. 262*, 12054−12058.
14. Cascieri, M. A., Chicchi, G. G., Applebaum, J., Hayes, N. S., Green, B. G., and Bayne, M. L. (1988) Mutants of Human Insulin-Like Growth Factor-I with Reduced Affinity for the Type-1 Insulin-Like Growth-Factor Receptor, *Biochemistry 27*, 3229−3233.
15. Tager, H. S. (1990) Mutant human insulins and insulin structure−function relationships, in *Handbook of Experimental Pharmacology* (Cuatrecasas, P., and Jacobs, S., Eds.) pp 41−64, Springer-Verlag, Berlin.
16. De Meyts, P., and Whittaker, J. (2002) Structural biology of insulin and IGF1 receptors: Implications for drug design, *Nat. Rev. Drug Discovery 1*, 769−783.
17. Adams, T. E., Epa, V. C., Garrett, T. P., and Ward, C. W. (2000) Structure and function of the type 1 insulin-like growth factor receptor, *Cell. Mol. Life Sci. 57*, 1050−1093.
18. Soos, M., Field, C. E., and Siddle, K. (1993) Purified hybrid insulin/insulin-like growth factor-I receptors bind insulin-like growth factor-I, but not insulin, with high affinity, *Biochem. J. 290*, 419−426.
19. Bayne, M. L., Applebaum, J., Chicchi, G. G., Hayes, N. S., Green, B. G., and Cascieri, M. A. (1988) Structural Analogs of Human Insulin-Like Growth Factor-I with Reduced Affinity for Serum Binding-Proteins and the Type-2 Insulin-Like Growth-Factor Receptor, *J. Biol. Chem. 263*, 6233−6239.
20. Young, J. D., and Carpenter, F. H. (1961) Isolation and characterization of products formed by the action of trypsin on insulin, *J. Biol. Chem. 236*, 743−748.
21. Inouye, K., Watanabe, K., Morihara, K., Tochino, Y., Kanaya, T., Sakibara, S., and Emura, J. (1979) Enzyme-Assisted Semisynthesis of Human Insulin, *J. Am. Chem. Soc. 101*, 751−752.
22. Kubiak, T., and Cowburn, D. (1986) Enzymatic semisynthesis of porcine despentapeptide (B26−30) insulin using unprotected desoctapeptide (B23−30) insulin as a substrate. Model studies, *Int. J. Pept. Protein Res. 27*, 514−521.
23. Svoboda, I., Brandenburg, D., Barth, T., Gattner, H. G., Jiracek, J., Velek, J., Blaha, I., Ubik, K., Kasicka, V., and Pospisek, J. (1994) Semisynthetic insulin analogues modified in positions B24, B25 and B29, *Biol. Chem. Hoppe-Seyler 375*, 373−378.
24. Zorad, S., Golda, V., Fickova, M., Macho, L., Pinterova, L., and Jurcovicova, J. (2002) Terguride treatment attenuated prolactin release and enhanced insulin receptor affinity and GLUT 4 content in obese spontaneously hypertensive female, but not male rats, *Ann. N.Y. Acad. Sci. 967*, 490−499.
25. Leslie, A. G. W. (1992) Recent changes to the MOSFLM package for processing film and image plate data, *CCP4 and ESF-EACMB Newsletter on Protein Crystallography*, Number 26.
26. Smith, G. D., Ciszak, E., Magrum, L. A., Pangborn, W. A., and Blessing, R. H. (2000) R6 Hexameric Insulin Complexed with m-Cresol or Resorcinol, *Acta Crystallogr. D56*, 1541−1548.
27. Vagin, A., and Teplyakov, A. (1997) MOLREP: An automated program for molecular replacement, *J. Appl. Crystallogr. 30*, 1022−1025.
28. Navaza, J. (1994) AMoRe: An automated package for molecular replacement, *Acta Crystallogr. A50*, 157−163.
29. Murshudow, G. N., Vagin, G. N., and Dodson, E. J. (1997) Refinement of macromolecular structures by the maximum likelihood method, *Acta Crystallogr. D57*, 122−133.
30. Lamzin, V. S., and Wilson, K. S. (1993) Automated refinement of protein models, *Acta Crystallogr. D49*, 129−149.
31. Collaborative Computational Project Number 4 (1994) *Acta Crystallogr. D50*, 760−763.
32. Kraulis, P. J. (1991) MOLSCRIPT: A Program to produce both detailed and schematic plots of protein structures, *J. Appl. Crystallogr. 24*, 946−950.
33. Laskowski, R. A., MacArthur, M. W., Moss, D. S., and Thornton, J. M. (1993) *PROCHECK*: A program to check the stereochemical quality of protein structures, *J. Appl. Crystallogr. 26*, 283−291.
34. Cosmatos, A., Frederigos, N., and Katsoyannis, P. G. (1979) Chemical synthesis of [des(tetrapeptide B27−B30), Tyr(NH2)-26-B] and [des(pentapeptide B26−B30) human (porcine) insulin, *J. Chem. Soc., Perkin Trans. 1 11*, 1311−1317.
35. Fischer, W. H., Saunders, D., Brandenburg, D., Wollmer, A., and Zahn, H. (1985) A shortened insulin with full in vitro potency, *Biol. Chem. Hoppe-Seyler 366*, 521−525.
36. Wollmer, A., Gilge, G., Brandenburg, D., and Gattner, H. G. (1994) An insulin with the native sequence but virtually no activity, *Biol. Chem. Hoppe-Seyler 375*, 219−222.
37. Kurapkat, G., De Wolf, E., Grotzinger, J., and Wollmer, A. (1997) Inactive conformation of insulin despite its wild-type sequence, *Protein Sci. 6*, 580−587.
38. Nakagawa, S. H., Johansen, N. L., Madsen, K., Schwartz, T. W., and Tager, H. S. (1993) Implications of replacing peptide bonds in the COOH-terminal B-chain domain of insulin by the ψ (CH2−NH) linker, *Int. J. Pept. Protein Res. 42*, 578−584.
39. Smith, G. D., and Dodson, G. G. (1992) The structure of rhombohedral R6 insulin hexamer that binds phenol, *Biopolymers 32*, 441−445.
40. Wan, Z.-l., Xu, B., Chu, Y.-C., Katsoyannis, P. G., and Weiss, M. (2003) Crystal structure of allo-IleA2-Insulin, an inactive chiral analogue: Implications for the mechanism of receptor binding, *Biochemistry 42*, 12770−12783.
41. Howey, D. C., Bowsher, R. R., Brunelle, R. L., and Woodworth, J. R. (1994) [Lys(B28), Pro(B29)]-human insulin. A rapidly absorbed analogue of human insulin, *Diabetes 43*, 396−402.

BI048856U